Device concepts based on spin-dependent transmission in semiconductor heterostructures

D. Z.-Y. Ting[1] and X. Cartoixà[2,*]

[1] *Jet Propulsion Laboratory, California Institute of Technology, Pasadena, CA 91109, USA*
[2] *Dept. of Physics, U. Illinois at Urbana-Champaign, Urbana, IL 61801, USA*

ABSTRACT

We examine zero-magnetic-field spin-dependent transmission in nonmagnetic semiconductor heterostructures with structural inversion asymmetry (SIA) and bulk inversion asymmetry (BIA), and report spin devices concepts that exploit their properties. Our modeling results show that several design strategies could be used to achieve high spin filtering efficiencies. The current spin polarization of these devices is electrically controllable, and potentially amenable to high-speed spin modulation, and could be integrated in optoelectronic devices for added functionality.

Key Words: Spin filter, Rashba effect, resonant tunneling, bulk inversion asymmetry

Running Tilte: semiconductor heterostructure spin devices ...

1. INTRODUCTION

Spin degeneracy in non-magnetic semiconductor heterostructures results from time reversal and spatial inversion symmetries, and can be lifted by spin-orbit interaction in the presence of structural inversion asymmetry (SIA) or bulk inversion asymmetry (BIA). SIA- and BIA-induced spin splittings can be described by the Rashba effect [1] and the Dresselhaus term [2], respectively. They can be exploited to build spin devices using only non-magnetic semiconductor heterostructures, without external magnetic fields or optical excitation. Nonmagnetic semiconductor heterostructure spin device concepts originated with the resonant tunneling spin filter proposed by Voskoboynikov *et al.* [3]. Subsequently, a number of new device concepts have emerged, including the triple-barrier resonant tunneling diode (TB-RTD) [4], the asymmetric resonant interband tunneling diode (aRITD) [5,6], the bi-directional resonant tunneling spin pump [7], and the [110]-RITD [8]. In this paper we present an overview and modeling results on some of these concepts, and discuss their prospects.

2. DEVICE CONCEPTS

We illustrate the concept of nonmagnetic heterostructure spin filters using the asymmetric resonant tunneling structure (aRTS) as an example. Quantized states in aRTS are spin-split by the Rashba effect [1]. Spin filtering is accomplished by exploiting the phenomenon that the spin of a resonantly transmitted electron aligns with that of the quasibound state traversed [3, 9]. Figure 1(a) illustrates the properties of quasibound quantum well states in an aRTS. Rashba effect induced spin splitting in the lowest conduction band (cb1) states are shown in the left panel. The shaded disks in the right panel are $\mathbf{k}_{\|}$-space representations of available quasibound states with energy below the incident electron reservoir Fermi level. These are the states that participate in resonant tunneling, and their spin directions determine the spin polarization of the transmitted electrons in the collector. When the spin directions of two spin-split subbands are plotted along the disk perimeters, they appear in counter-clockwise (ccw) and clockwise (cw) pinwheel patterns. Thus we label the subbands "ccw" and "cw." Note that ccw and cw subband states at the same $\mathbf{k}_{\|}$ have opposite spins, and that states with opposite $\mathbf{k}_{\|}$ within a given subband have opposite spins. Thus, to achieve efficient spin filtering we must provide mechanisms for (1) preferentially selecting a particular spin-split subband, and (2) lateral momentum selection.

2.1. Subband Filtering

The subband filtering efficiency is defined as $\eta = (J_{ccw}-J_{cw})/(J_{ccw}+J_{cw})$, where J_{ccw} and J_{cw} are the resonant tunneling current density components associated with the ccw and cw subband tunneling, respectively. In the aRTS η is typically limited by cancellation between the ccw and cw subband contributions. The strategy for optimizing η is to increase spin splitting, thereby enlarging the difference between ccw and cw contributions. One way to strengthen the selectivity between the ccw and cw subbands is to use the spin-blockade mechanism proposed by Koga *et al.* [4]. Their proposed device consists of a triple-barrier structure containing back-to-back asymmetric wells coupled through a thin central tunneling barrier. The two quantum wells have opposite ordering of the ccw and cw subbands. Resonant tunneling is blocked unless the quasibound state spins in the two wells are aligned (spin blockade). Either ccw-ccw or cw-cw alignment can be selected by the biasing voltage. This technique has resulted in very high calculated subband filtering efficiency of $\eta > 99.9\%$ [4]. Alternatively, we can improve spin filtering efficiency by exploiting the strong spin-dependent interband tunneling through valence band states in asymmetric resonant interband tunneling diodes (aRITDs) [5]. The interband design uses large valence band spin-orbit interaction to provide strong spin selectivity, but does not leave the electrons in valence bands where spin relaxation is fast. Filtering efficiency is also enhanced by the reduction of tunneling through quasibound states near the zone center. Another interband device concept takes advantage of bulk inversion asymmetry (BIA) induced spin splitting in (110) devices to perform spin filtering [8].

2.2. Lateral Momentum Selection

Lateral momentum selection can be accomplished in several ways. Voskoboynikov *et al.* proposed using a small in-plane electric field in the source region of the aRTS to shift the incident electron distribution towards, say, the positive k_x side in k-space [3]. Figure 1(b) shows that a lateral E-field along the x direction would result in net $+y$ and $-y$ spin polarizations for resonant tunneling currents transmitted through the ccw and cw subbands, respectively. And since cw subband current contributions are larger, the total transmitted current yields a net $-y$ current spin polarization. Note that, as indicated in Fig. 1(c), reversing the direction of the lateral E-field causes the collector current to be spin polarized in the opposite direction. Thus, it is possible to modulate the spin polarization by changing the direction of the lateral E-field. A variant lateral E-field scheme, proposed by Chow and Moon [6], uses lateral side-gates fabricated on the mesa sidewalls of the resonant tunneling structure. The side gates are electrically isolated from the mesa itself, and do not induce a lateral current in the emitter region. An alternative for creating lateral momentum anisotropy was proposed by Datta and co-workers [4]. It makes use of a one-sided collector, which is placed on, for example, the positive x side to collect only electrons with positive k_x. As illustrated schematically in Fig. 1(d), the ensemble of electrons transmitted through the ccw (cw) subband has a net spin polarization along the positive (negative) y direction. It can be shown that for the one-sided collector geometry, the net current spin polarization, $P = (J_{+y} - J_{-y})/(J_{+y} + J_{-y})$, where J_{+y} and J_{-y} are resonant tunneling current density components spin polarized along the positive and negative y directions, respectively, is related to the subband filtering efficiency in a simple manner when we consider SIA only: $P = (2/\pi)\eta$ [10]. This limits P to a theoretical maximum of $(2/\pi) \approx 63.7\%$ for the one-sided collector geometry.

2.3. Bi-Directional Spin Pump

Much of the effort in designing the resonant tunneling spin filters goes into circumventing the problem caused by the fact that quasibound states with opposite $\mathbf{k}_{\|}$ within a given subband have opposite spins. Rather than avoiding this problem, the bi-directional spin-pump [7] is design to take advantage of this property. A bi-directional spin-pump is similar in structure to the resonant tunneling spin filter. In the spin pump, we do not intentionally bias the device along the growth (z) direction, but apply a small lateral E-field in the emitter region only. Consider a spin pump structure where the emitter and the collector are made from the same material and doped to equal carrier concentrations. As illustrated in Fig. 2, the application of an in-plane E-field along the x direction displaces the emitter Fermi surface. It creates an excess of carriers on the $+k_x$ side, which can tunnel to the collector, and a deficit of carriers on the $-k_x$ side, which becomes available to receive electrons tunneling back from the collector. Provided that the spin filter structure has high subband filtering efficiency, and assuming (without loss of generality) that it is designed such that resonant tunneling through the cw states dominates over the ccw states at zero bias, then resonantly transmitted electrons on the $+k_x$ and $-k_x$ sides will be spin polarized along the $-y$ and $+y$ directions, respectively. This results in a forward (emitter to collector) electron (particle) current with $-y$ spin polarization, and a backward current with $+y$

spin polarization, as illustrated in Fig. 2. The bi-directional spin pump induces the simultaneous flow of oppositely spin-polarized current components in opposite directions, and can thus generate significant levels of spin current with very little net electrical current across the tunnel structure, a condition characterized by current spin polarization in excess of 100%. Incidentally, the accumulation of spins in the bi-directional spin pump is reminiscent of the spin Hall effect [11], and may thus be analyzed in that framework.

2.4. Enhancement from Bulk Inversion Asymmetry Effects

The resonant tunneling spin filter and spin pump concepts were developed to exploit the Rashba effect [1], which is a consequence of spin–orbit interaction and the presence of structural inversion asymmetry (SIA). The effect on spins due to the presence of bulk inversion asymmetry (BIA) in zincblende semiconductors can also be exploited for spin device applications. It can be shown that the efficiency of nonmagnetic resonant tunneling spin devices can be improved significantly when SIA and BIA effects are combined properly [10]. The design modifications required to take advantage of this improvement are minimal: we only need to be specific in selecting the direction of one-sided collectors or the lateral E-field with respect to the crystallographic orientation of the heterostructure [10].

The consideration of the interplay between SIA and BIA effects has also led us to a new device concept based on considerations of spin lifetime tuning. The resonant spin lifetime transistor (RSLT) [12,13] concept is reported elsewhere in this issue.

3. MODELING RESULTS

In this section we present spin filter modeling results, calculated using the multiband quantum transmitting boundary method [14], on asymmetric resonant tunneling structure (aRTS), an asymmetric resonant interband tunneling diode (aRITD), and a spin blockade triple barrier resonant tunneling diode (TB-RTD), all constructed in the nearly-lattice-matched InAs/GaAs/AlSb material system. Device schematic band diagrams are illustrated in Fig. 3. Band structure is described by the effective bond orbital model [15], using typical 8-band $\boldsymbol{k}\cdot\boldsymbol{p}$ material parameters taken from the literature. Figure 4, 5, and 6 respectively show the calculated results for aRTS, aRITD, and TB-RTD. In each figure, the left panel shows the results for the case with applied lateral E-field in the emitter. Spin polarized current density components J_{+y} and J_{-y} are shown on the top, and the current spin polarization in the bottom. The right panel shows the computed subband current densities J_{ccw} and J_{cw} on top, and one-sided collector current spin polarization P as functions of applied bias on the bottom.

Figure 4 shows that the subband filtering efficiency in the aRTS is typically limited to low values, resulting from cancellation between the ccw and cw subband contributions. Note in Fig. 1 that the minima of the lower spin-split subband are located away from $\mathbf{k}_{\|}=0$, and are below the upper subband minimum at $\mathbf{k}_{\|}=0$. Significant levels of subband filtering efficiency can be obtained in the special case when the emitter Fermi level is located in the small energy window between the lower and upper subband minima. This can occur at the onset of resonant tunneling (~ 0.88 V in Fig. 4), typically with low current densities, however.

Figure 5 show that substantially higher current spin polarization can be obtained in the aRITD. The one-sided collector result on the right in Fig. 5 shows that the aRITD can be a highly efficient spin filter, with P approaching the theoretical maximum one-sided collector efficiency of 63.7% near 0.025 V at relatively large current density levels. Note also that there is no net current spin polarization at the peak of the J-V curves near 0.11 V. This is because the peak is dominated by the light-hole 1 (lh1) resonant tunneling process, which favors contributions from the zone-center, where Rashba spin splitting vanishes. At below 0.05V, heavy-hole 1 (hh1) tunneling dominates. Here the away-from-zone-center resonant tunneling processes, which show strong spin dependence, are favored. Note that in the lateral E-field case, as the applied bias approaches 0, the collector current spin polarization becomes greater than 1. This is a manifestation of the bi-directional spin pump effect [7].

Fig. 6 shows that the spin-blockade TB-RTD also can achieve near theoretical maximum one-sided collector spin polarization when the quasibound states in the two back-to-back asymmetric quantum wells are biased to ccw-ccw (~0.01V) or cw-cw (~ -0.01V) alignment. As with the aRITD, with near zero vertical bias and a finite applied lateral E-field, the TB-RTD can achieve current spin polarization > 100%. Note that the two current peaks favoring opposite spin polarization are quite close to each other, separated only by 0.02 V in this case.

4. DISCUSSIONS

The concept of non-magnetic heterostructure spin filters is still being refined. Here we point out a few areas that are under development. A common assumption used in the resonant tunneling spin filter models thus far is coherent tunneling. This preserves the lateral momentum anisotropy during the resonant tunneling process, so that net spin polarization can be obtained in the collector. Coherent tunneling is more likely to occur when resonant tunneling lifetimes are shorter than typical scattering times in the quantum well. For the aRITD structure studied in Fig. 5, the typical tunneling lifetime is on the order of 10 ps. Studies in designing spin-dependent tunneling devices with shorter tunneling lifetimes are ongoing. There has been indirect evidence for the demonstration of coherent tunneling in large-current density resonant tunneling devices [16]. It should be noted that coherent tunneling is a sufficient, but not a necessary requirement for the resonant tunneling spin filter. More detailed studies of the dynamics of spin transport in resonant tunneling spin filters are needed for better understanding.

Another issue being study currently is the effect of higher order *k* terms. We have shown that BIA effects can be used to enhance spin filtering efficiencies using a model Hamiltonian that describes linear-in-*k* spin splitting for states near the zone center [10]. The recent work of Winkler points out that the quantum well state spin directions can be more complex when higher-order *k* terms are included [17], and we expect the higher-order *k* terms to have important effects for transport as well. These effects are being studied using a band structure method that incorporates BIA effects in the eight-band effective bond orbital model (BIA-EBOM) [18].

A salient feature of the non-magnetic semiconductor heterostructure spin devices is that they do not need magnetic elements (e.g. Mn), and are compatible with conventional semiconductor growth technology. This means that they can be grown, for instance, in the same molecular beam epitaxy machine that is used to grow lasers, detectors, or transistors. However, the need for lateral momentum selection means that they require sophisticated device design and processing technology, such as those used in the fabrication of the split side-gated resonant interband tunneling devices [19].

A resonant tunneling spin filter implemented in the lateral E-field geometry (including split side gate) offers us the ability to control the current spin polarizations electrically, as illustrated in Fig. 1(b) and 1(c). Therefore it is potentially amenable to high-speed spin modulation through electrical means, such as side-gate voltage modulation. A possible application for a spin polarized current source, capable of being modulated electrically at high speeds, is the electrically pumped spin VECSL [20]. In the "spin laser" light polarization follows modulation in injected carrier spin, and can carry information in both light polarization and intensity.

5. SUMMARY

We reported progress on the development of device concepts that exploit spin-orbit coupling for creating spin polarized current sources using nonmagnetic semiconductor resonant tunneling heterostructures, without external magnetic fields. These spin polarized current source are potentially capable of being modulated electrically at high speeds, and could be useful for spintronics and spin-optoelectronics applications.

ACKNOWLEDGMENTS

The authors thank O. Voskoboynikov, A. T. Hunter, D. L. Smith, D. H. Chow, J. S. Moon, T. C. McGill, T. F. Boggess, J. N. Schulman, P. Vogl, T. Koga and Y.-C. Chang for discussions. This work was sponsored by the DARPA SpinS Program through HRL Laboratories. A part of this work was carried out at the Jet Propulsion Laboratory, California Institute of Technology, through an agreement with the National Aeronautics and Space Administration.

* Present address: Computational Research Division, Lawrence Berkeley National Laboratory, Berkeley, CA 94720, USA

Reference:

1. Y. A. Bychkov and E. I. Rashba, *J. Phys. C - Solid State Phys.* **17**, 6039 (1984).
2. G. Dresselhaus, *Phys. Rev.* **100**, 580-6 (1955).
3. A. Voskoboynikov, S. S. Lin, C. P. Lee, and O. Tretyak, *J. Appl. Phys.* **87**, 387 (2000).

4. T. Koga, J. Nitta J, H. Takayanagi, and S. Datta, *Phys. Rev. Lett.* **88** 12661 (2002).
5. D. Z-Y. Ting and X. Cartoixà, *Appl. Phys. Lett.* **81**, 4198 (2002).
6. D. Z-Y. Ting, X. Cartoixà, D. H. Chow, J. S. Moon, D. L. Smith, T. C. McGill and J. N. Schulman, *IEEE Proceedings* **91** 741 (2003).
7. D. Z-Y. Ting and X. Cartoixà, *Appl. Phys. Lett.* **83**, 1391 (2003).
8. K. C. Hall, W. H. Lau, K. Gundogdu, M. E. Flatte and T. F. Boggess, *Appl. Phys. Lett.* **83**, 2937 (2003).
9. E. A. de Andrada e Silva and G. C. La Rocca, *Phys. Rev. B* **59**, 15583 (1999).
10. D. Z.-Y. Ting and X. Cartoixà, *Phys. Rev. B* **68**, 235320 (2003).
11. J. E. Hirsch, *Phys. Rev. Lett.* **83**, 1834 (1999).
12. X. Cartoixà, D. Z.-Y. Ting and Y.-C. Chang, *Appl. Phys. Lett.* **83**, 1462 (2003).
13. X. Cartoixà, D. Z.-Y. Ting and Y.-C. Chang, *cond-mat*/0402237 (2004).
14. D. Z.-Y. Ting, E. T. Yu, and T. C. McGill, *Phys. Rev. B* **45**, 3583 (1992).
15. Y.-C. Chang, *Phys. Rev. B* **37**, 8215 (1988).
16. R. C. Bowen, G. Klimeck, R. K. Lake, W. R. Frensley, and T. Moise, *J. Appl. Phys.* **81**, 3207 (1997); W. R. Frensley, private communications.
17. R. Winkler, *Phys. Rev. B* **69**, 045317 (2004).
18. X. Cartoixà, D. Z.-Y. Ting, and T. C. McGill, *Phys. Rev. B* **68**, 235319 (2003).
19. J. S. Moon et al., to appear in *Appl. Phys. Lett.* (2004).
20. M. Oestreich, M. Bender, J. Hubner, D. Hagele, W. W. Ruhle, T. Hartmann, P. J. Klar, W. Heimbrodt, M. Lampalzer, K. Volz, W. Stolz, *Semicond. Sci. Technol.* **17**, 285 (2002).

Figure Captions:

Figure 1. (a) Lowest conduction subband (cb1) in an asymmetric quantum well showing Rashba spin splitting. Available quasibound states in the cb1 with energy below the emitter Fermi level are shown as shaded disks in $\mathbf{k}_{\|}$-space. Arrows indicate spin directions. (b) Same as (a), but with the Fermi surface in the incidence electrode displaced by the application of a lateral E-field along the x direction. (c) Same as (b), but with the lateral E-field in the opposite direction, resulting in the opposite net spin polarization. (d) Depiction of states collected by a one-sided collector located on the positive *x* side.

Figure 2. Schematic illustration of the emitter and collector reservoirs in a bi-directional spin pump structure. A lateral E-field is applied to the emitter, but not the collector.

Figure 3. Schematic band diagrams of (a) asymmetric resonant tunneling structure, (b) an asymmetric resonant interband tunneling diode, and (c) a spin blockade triple barrier resonant interband tunneling diode.

Figure 4. Calculated current density components (top) and current polarization efficiencies (bottom) as functions of applied bias for an asymmetric resonant tunneling structure (aRTS). The left and right panels show the results for the lateral E-field and the one-sided collector geometries, respectively.

Figure 5. Calculated current density components (top) and current polarization efficiencies (bottom) as functions of applied bias for an asymmetric resonant interband tunneling diode (aRITD). The left and right panels show the results for the lateral E-field and the one-sided collector geometries, respectively.

Figure 6. Calculated current density components (top) and current polarization efficiencies (bottom) as functions of applied bias for a triple barrier spin blockade structure. The left and right panels show the results for the lateral E-field and the one-sided collector geometries, respectively.

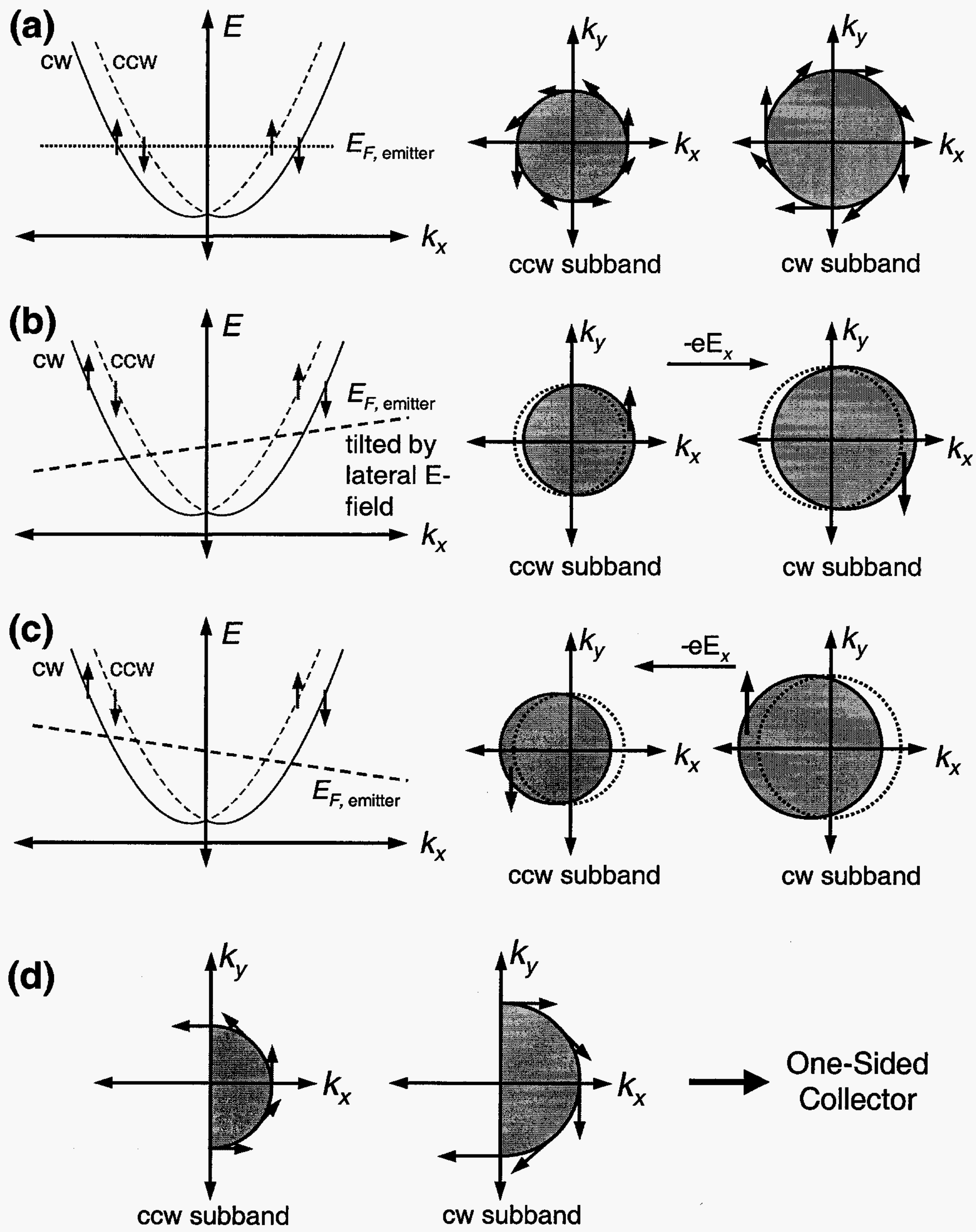

Figure 1. Ting and Cartoixà.

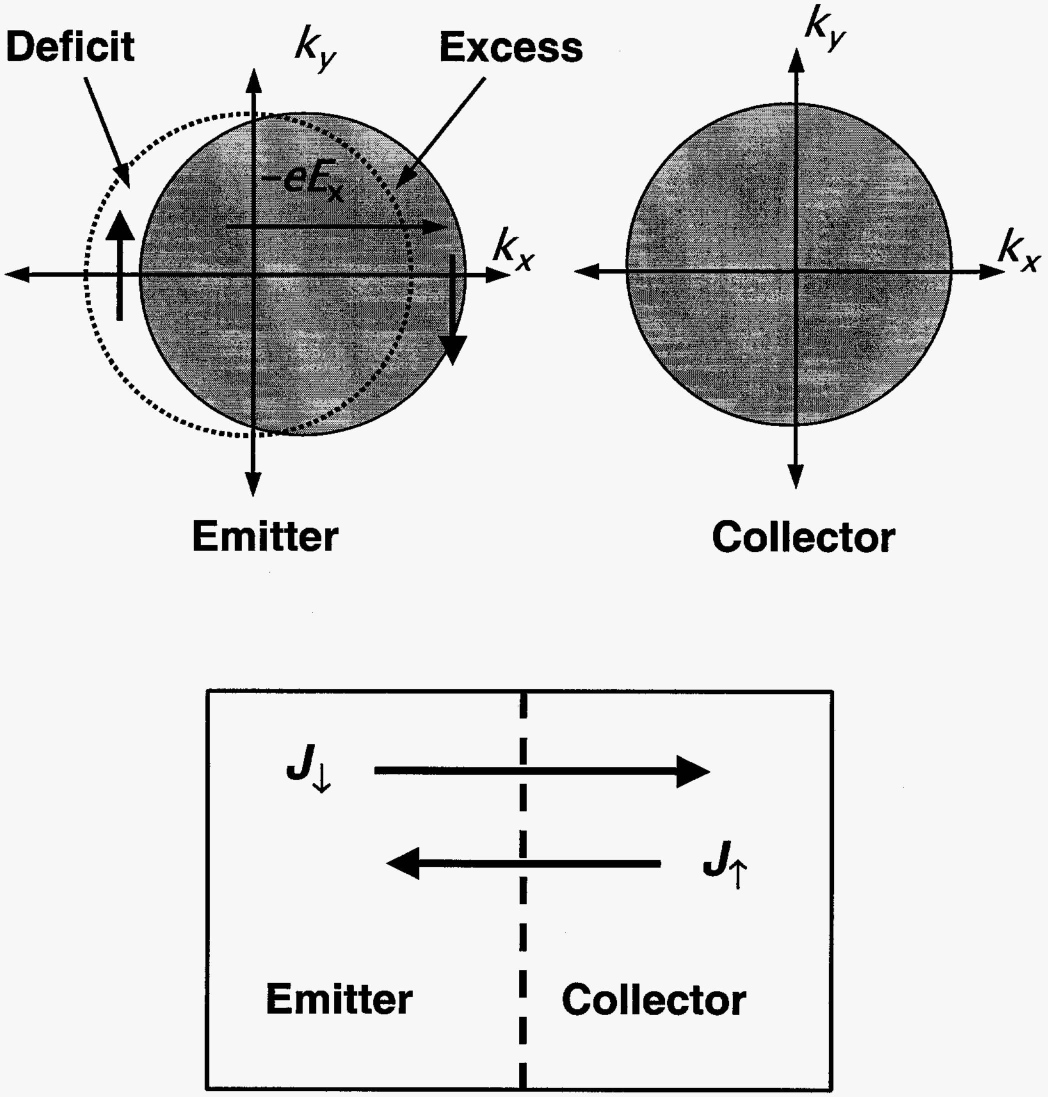

Figure 2. Ting and Cartoixà.

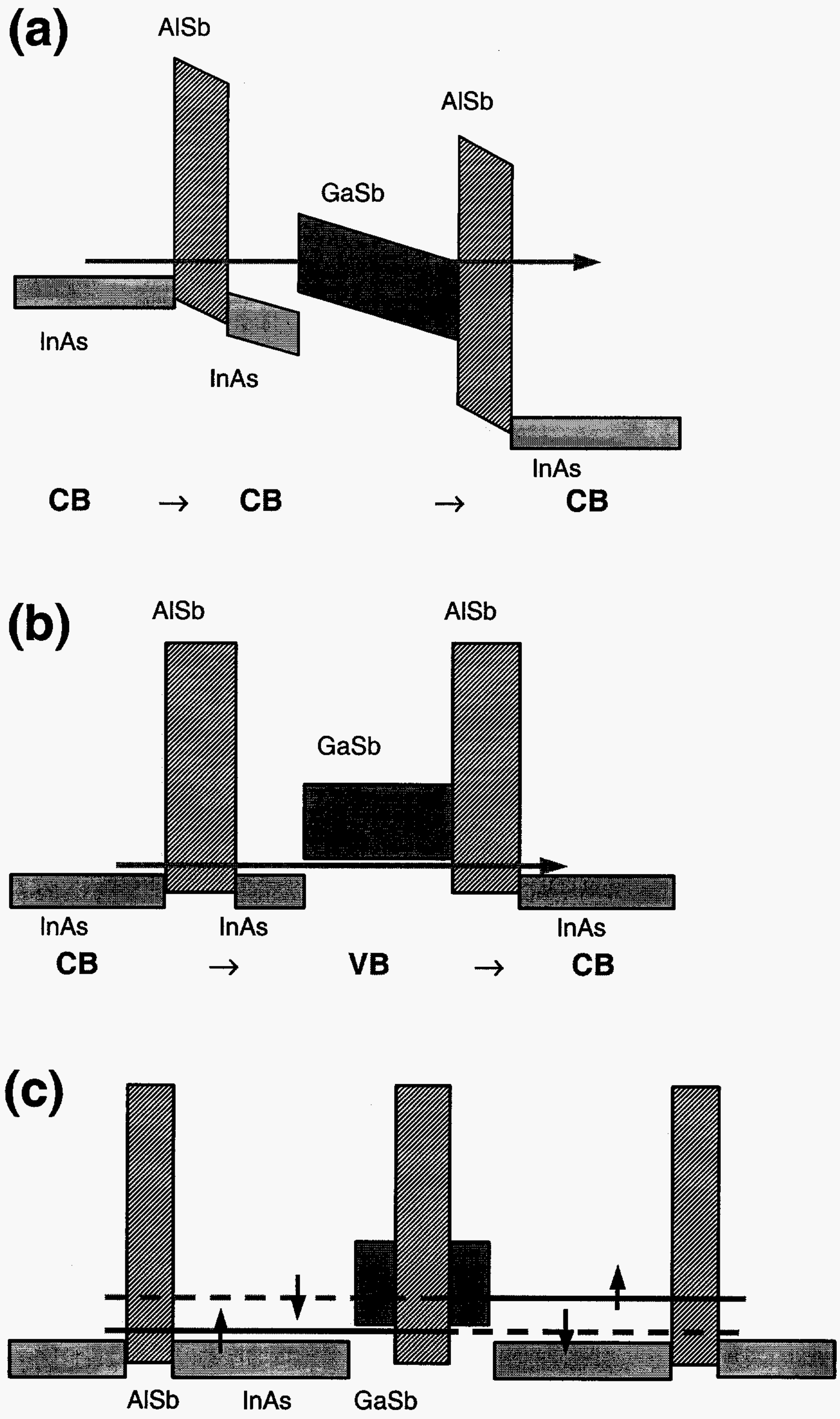

Figure 3. Ting and Cartoixà.

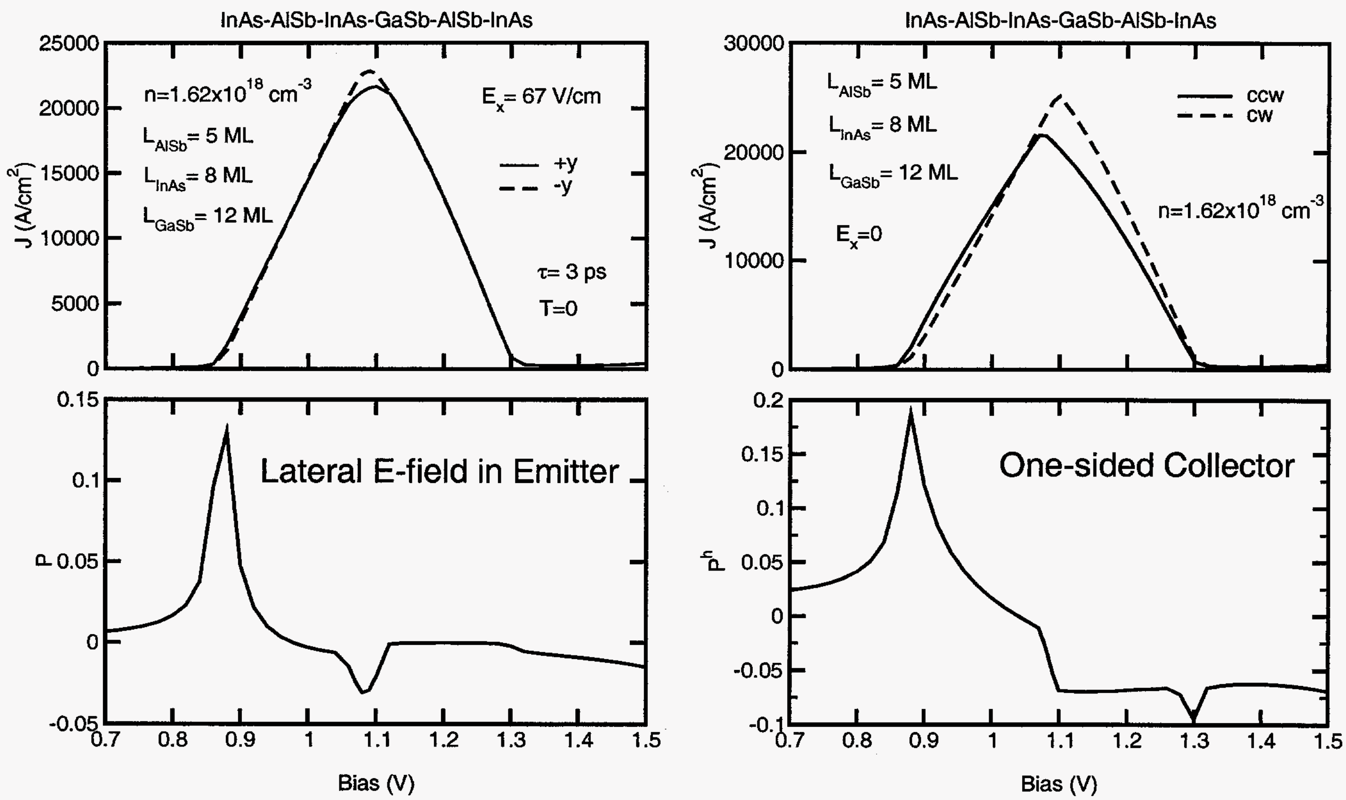

Figure 4. Ting and Cartoixà.

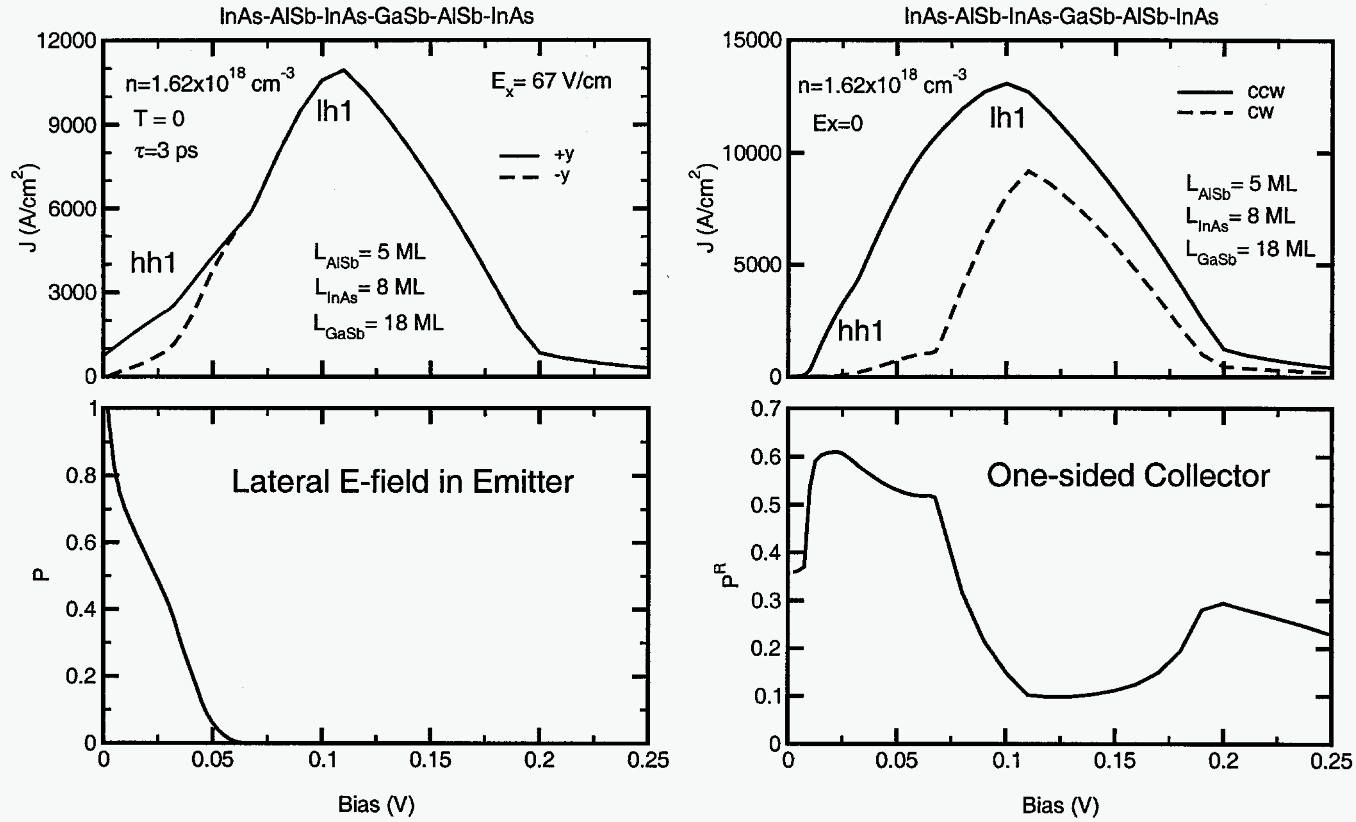

Figure 5. Ting and Cartoixà.

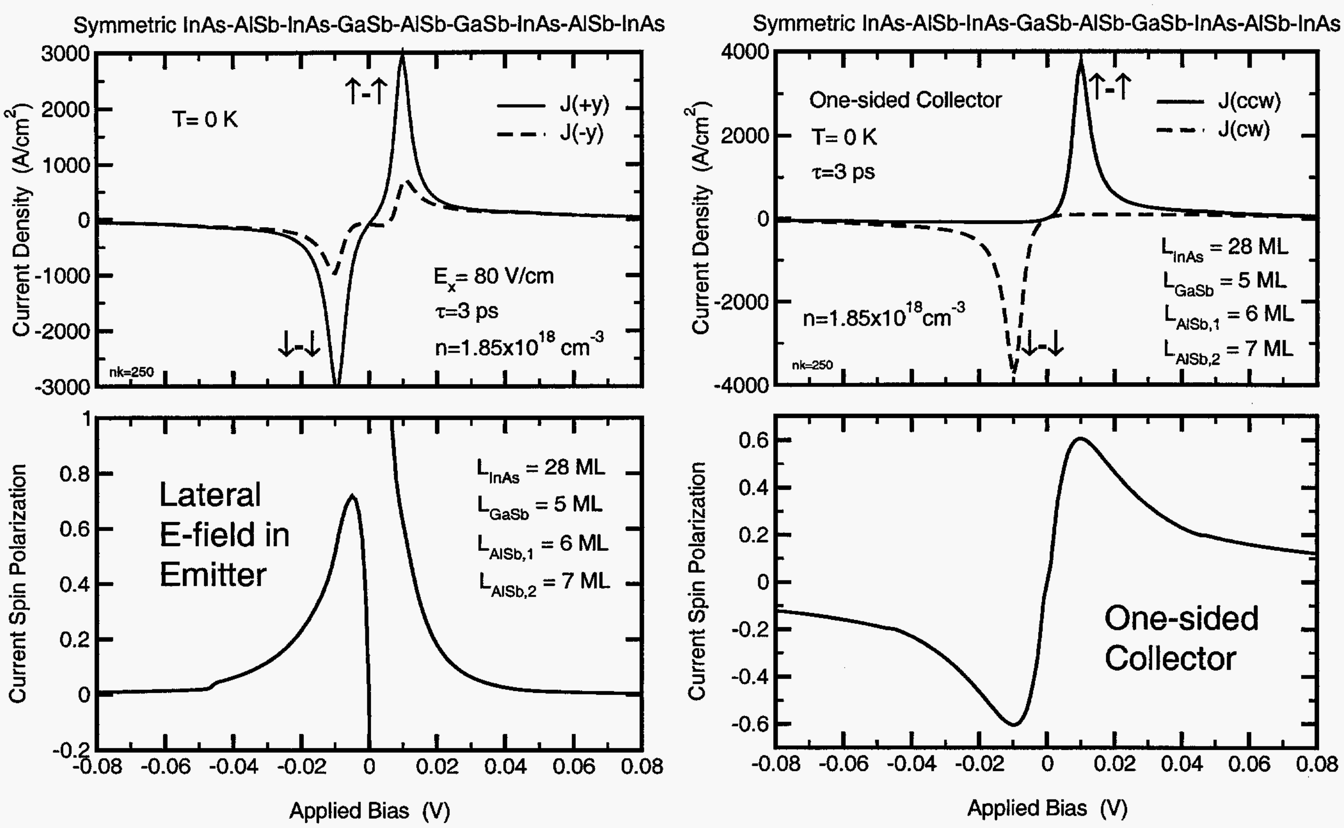

Figure 6. Ting and Cartoixà.